PROCEEDINGS OF SCIENCE

Jet measurements in pp, p–Pb and Pb–Pb collisions with ALICE at the LHC

S. K. Prasad[*][†]
Centre for Astroparticle Physics and Space Science, Bose Institute, Kolkata, 700091 (INDIA)
E-mail: sprasad@cern.ch

We present a systematic study of jet measurements in pp, p–Pb and Pb–Pb collisions using the ALICE detector at the LHC. Jet production cross sections are measured in pp collisions at $\sqrt{s}$ = 2.76 and 7 TeV, in p–Pb collisions at $\sqrt{s_{\rm NN}}$ = 5.02 TeV and in Pb–Pb collisions at $\sqrt{s_{\rm NN}}$ = 2.76 TeV. Jet shape observables and fragmentation distributions are measured in pp collisions at 7 TeV. Jets are reconstructed at midrapidity in a wide range of transverse momentum using sequential recombination jet finding algorithms ($k_{\rm T}$, anti-$k_{\rm T}$, and SISCone) with several values of jet resolution parameter R in the range 0.2 – 0.6. Measurements are compared to Next-to-Leading Order (NLO) perturbative Quantum Chromodynamics (pQCD) calculations and predictions from Monte Carlo (MC) event generators such as PYTHIA, PHOJET and HERWIG. Jet production cross sections are well reproduced by NLO pQCD calculations in pp collisions at $\sqrt{s}$ = 2.76 TeV. MC models could not explain the jet cross sections in pp collisions at $\sqrt{s}$ = 7 TeV, whereas jet shapes and fragmentation distributions are rather well reproduced by these models. The jet nuclear modification factor $R_{\rm pPb}$ in p–Pb collisions is found to be consistent with unity indicating the absence of large modifications of the initial parton distribution or strong final state effects on jet production, whereas a large jet suppression is observed in Pb–Pb central events with respect to peripheral events indicating formation of a dense medium in central Pb–Pb events.

7th International Conference on Physics and Astrophysics of Quark Gluon Plasma
1-5 February , 2015
Kolkata, India

[*]Speaker.
[†]On behalf of the ALICE Collaboration.

PoS(ICPAQGP2015)088

1. Introduction

In high energy hadronic or nuclear collisions, hard (large momentum transfer Q^2) scattered partons (quarks and gluons) fragment and hadronize, resulting in a collimated shower of particles known as a jet [1]. Jet measurements in pp collisions provide a test of perturbative and non-perturbative aspects of jet production and fragmentation as implemented in the MC models, and form a baseline for similar measurements in nucleus–nucleus (A–A) and proton–nucleus (p–A) collisions. In A–A collisions an energetic parton while passing through the produced medium loses energy via induced gluon radiation and elastic scattering. Jet studies in A–A collisions in comparison to pp allow a better understanding of the medium induced modifications in the fragmentation of hard scattered partons and energy loss mechanisms [2, 3], whereas similar studies in p–A collisions potentially reveal the effects of (cold) nuclear matter (CNM). In this paper we present results of jet measurements obtained using ALICE detector in pp collisions at $\sqrt{s}$ = 2.76, 7 TeV, in p–Pb collisions at $\sqrt{s_{\mathrm{NN}}}$ = 5.02 TeV and in Pb–Pb collisions at $\sqrt{s_{\mathrm{NN}}}$ = 2.76 TeV.

2. Data sample, event selection, track selection, and jet reconstruction

The data used in this analysis were collected during the LHC run in 2010 for pp collisions at 7 TeV, in 2011 for pp collisions at 2.76 TeV, in fall of 2010 for Pb–Pb collisions, and in the beginning of 2013 for p–Pb collisions using the ALICE detector [4, 5]. Minimum bias events are selected based on information from Silicon Pixel Detector (SPD) [6] and V0 [7] detectors (V0A, V0C) [8, 9, 10, 11]. The Electromagnetic Calorimeter (EMCal) [12] is used in addition to select EMCal triggered events [8]. Information from the Time Projection Chamber (TPC) [13] and Inner Tracking System (ITS) [6] are used to select charged tracks using a hybrid approach as discussed in [8]. The reconstruction of neutral particles is performed using the Electromagnetic Calorimeter (EMCal) [8]. Charged tracks with transverse momentum $p_{\mathrm{T}}^{\mathrm{track}} > 0.15$ GeV/c at midrapidity ($|\eta^{\mathrm{track}}| < 0.9$) are used as input to jet reconstruction. In addition, for jets including neutral particles, EMCal clusters with energy greater than 0.3 GeV/c are considered. Jets are reconstructed using the infrared collinear safe sequential recombination algorithm anti-k_{T} [14]. In p–Pb and Pb–Pb collisions, the k_{T} [15, 16] algorithm is used for the estimation of background. Jets are reconstructed with several values of the resolution parameter R in the range 0.2 – 0.6. Jets reconstructed using charged particles only as input are referred to as *'charged jets'* whereas jets reconstructed using both charged and neutral particles as input are known as *'full jets'* hereafter.

3. Correction for detector effects and background

Measured distributions are corrected for the instrumental effects and presented at particle level. Corrections for the instrumental effects, such as limited track reconstruction efficiency and finite momentum resolution, are performed using the unfolding techniques [17, 18] for jet cross sections whereas jet shape and fragmentation observables are corrected using a bin-by-bin technique. A full detector simulation is performed using the PYTHIA 6.425 [19] event generator and GEANT3 [20] particle transport package. All observables are also corrected for the contamination from the sec-

PoS(ICPAQGP2015)088

ondary particles [1] and background [2]. The method for estimation and correction of background is however different in pp to that in p–Pb and Pb–Pb collisions (see [8, 9, 10, 11] for details). In case of p–Pb and Pb–Pb events, region to region fluctuations of the estimated average background density arising due to fluctuations in the particle multiplicity and momentum, elliptic flow etc., are considerable. Background fluctuations are corrected for on an statistical basis using unfolding techniques (see Sec. 2 of [11]). The corrected results are compared to that obtained from various MC event generators e.g. PYTHIA (tune Perugia-0, Perugia-2011, AMBT1), HERWIG, PHOJET and NLO pQCD calculations.

4. Results

4.1 Jet measurements in pp collisions

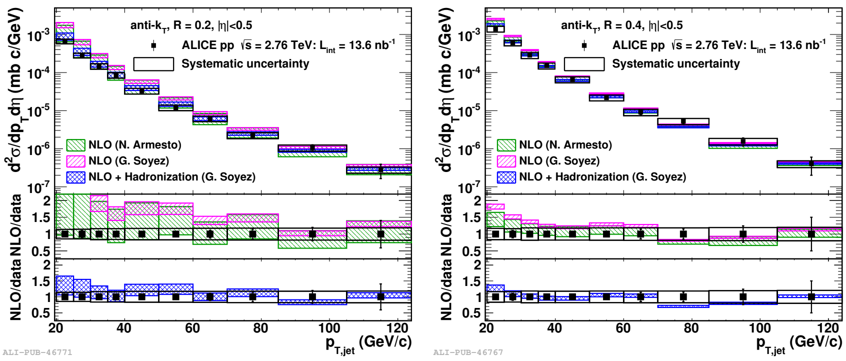

Figure 1: (Color online) Full jet production cross sections as a function of jet p_T compared to NLO pQCD calculations in pp collisions at $\sqrt{s}$ = 2.76 TeV for jets reconstructed with R = 0.2 (left) and 0.4 (right).

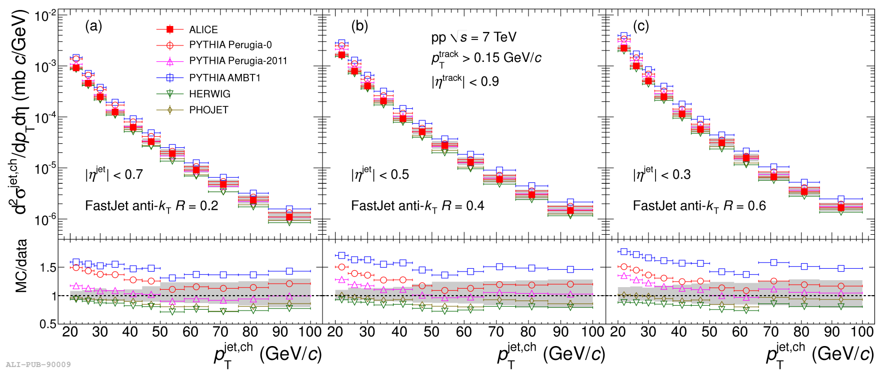

Figure 2: (Color online) Charged jet cross sections as a function of jet p_T compared to MC models in pp collisions at $\sqrt{s}$ = 7 TeV for jets reconstructed with R = 0.2 (left), 0.4 (middle) and 0.6 (right).

[1] Particles produced by weak decays and interactions of primary particles with detector material and beam pipe.
[2] Particles in an event which are not produced directly by hard scattering of partons.

The full jet production cross sections as a function of jet p_T compared to NLO pQCD calculations [21] are shown in Fig. 1 [8] for pp collisions at $\sqrt{s}$ = 2.76 TeV for jets reconstructed with R = 0.2 (left) and 0.4 (right). The NLO calculations reproduce the full jet cross sections reasonably well when hadronization effects are included. The charged jet cross sections compared to MC predictions, are shown in Fig. 2 for pp collisions at $\sqrt{s}$ = 7 TeV for R = 0.2 (left), 0.4 (middle) and 0.6 (right). None of the models can explain the data in the entire p_T range, the discrepancy being larger for larger R. The jet shape observables as defined by the radial transverse momentum density distributions about the jet axis as a function of distance 'r', jet constituents multiplicity and average radius containing 80% of jet p_T as a function of leading jet p_T, and the fragmentation distributions are, however, in general reasonably well reproduced by these models (figures not shown, see [9]).

4.2 Results from p–Pb and Pb–Pb collisions

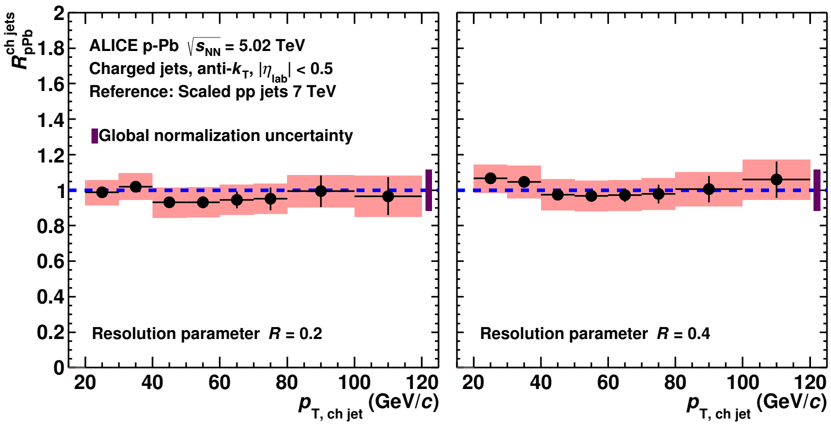

Figure 3: (Color online) Jet nuclear modification factors (R_{pPb}) in p–Pb collisions at $\sqrt{s_{NN}}$ = 5.02 TeV for charged jets reconstructed with R = 0.2 (left) and 0.4 (right).

The jet nuclear modification factor R_{pPb} [3] is shown in Fig. 3 for p–Pb collisions at $\sqrt{s_{NN}}$ = 5.02 TeV for charged jets reconstructed with R = 0.2 (left) and 0.4 (right). It is found to be consistent with unity in the measured p_T range indicating the absence of large modifications of the initial parton distribution or strong final state effects on jet production. The charged jet nuclear modification factor, R_{CP} [4] is shown in Fig. 4 as a function of jet p_T for three centrality bins for Pb–Pb collisions at $\sqrt{s_{NN}}$ = 2.76 TeV. A large jet suppression is observed in most central (0–10%) Pb–Pb collisions indicating the formation of a dense medium in such collisions. It is found to be centrality and p_T dependent. The left (right) panel of Fig. 5 shows ratios of spectra (cross sections) for jets measured with R = 0.2 and 0.4 (0.2 and 0.3) in p–Pb (Pb–Pb) collisions at $\sqrt{s_{NN}}$ = 5.02 TeV (2.76 TeV) compared to that obtained in pp collisions (PYTHIA). The ratio of jet spectra is sensitive to the collimation of particles around the jet axis and serves as an indirect measure of jet

[3] R_{pPb} is defined as the ratio of p_T spectra in p–Pb normalized by the nuclear overlap function $\langle T_{AA} \rangle$ obtained from Glauber model and pp cross section extrapolated to $\sqrt{s_{NN}}$ = 5.02 TeV.

[4] R_{CP} is defined as the ratio of jet p_T spectra in central and peripheral Pb–Pb collisions normalized by $\langle T_{AA} \rangle$ for each centrality class.

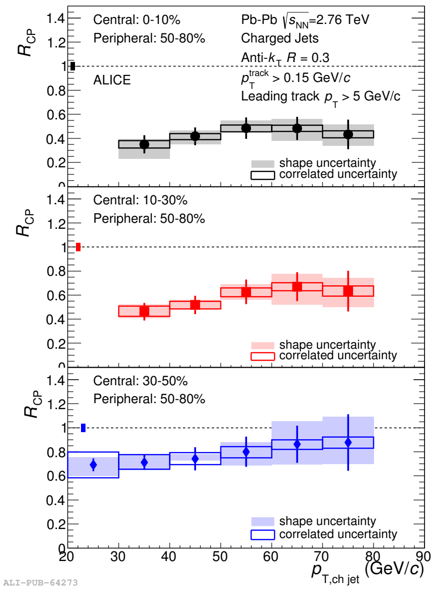

Figure 4: (Color online) Charged jet nuclear modification factors (R_{CP}) in Pb–Pb collisions at $\sqrt{s_{NN}}$ = 2.76 TeV for 0–10% (top), 10–30% (middle) and 30–50% (bottom) centrality classes.

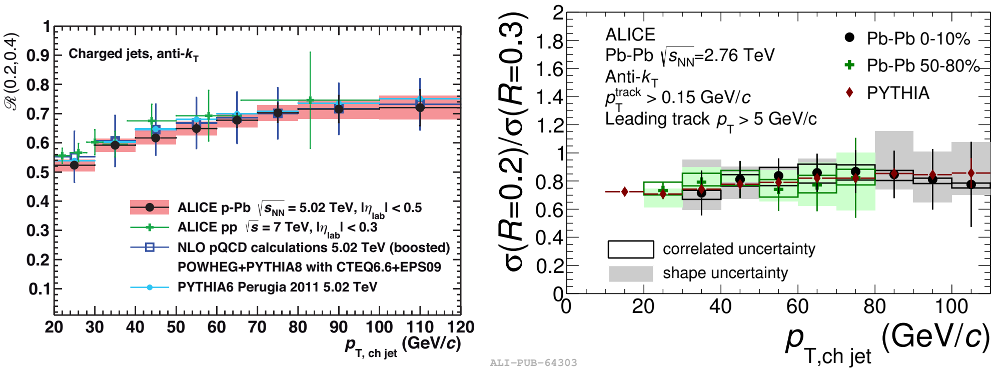

Figure 5: (Color online)The ratios of jet spectra measured with R = 0.2 to that obtained with larger R (0.4 for p–Pb and 0.3 for Pb–Pb) as a function of jet p_T in p–Pb (left) and Pb–Pb (right) collisions at 5.02 and 2.76 TeV respectively.

structure. In minimum bias p–Pb collisions the ratio of jet spectra is found to be compatible with that in pp collisions, PYTHIA and NLO pQCD calculations, and the cross section ratios in Pb–Pb is found to be similar for most central and peripheral collisions and compatible with PYTHIA indicating that the core of the jet within the measured R, remains unmodified in minimum bias p–Pb, peripheral Pb–Pb and even in most central Pb–Pb collisions.

5. Summary and conclusions

We reported jet measurements for pp, p–Pb and Pb–Pb collisions at various centre-of-mass energies using the ALICE detector. Jets are measured at midrapidity using the anti-k_T jet finding algorithm with several values of the jet resolution parameter (R in the range 0.2 to 0.6). Full jet cross sections are well reproduced by NLO pQCD calculations in pp collisions at $\sqrt{s}$ = 2.76 TeV. None of the MC models under study can explain the charged jet cross sections in pp collisions at $\sqrt{s}$ = 7 TeV, however jet shape observables and fragmentation distributions are rather well reproduced by these models. The jet nuclear modification factor for minimum bias p–Pb collisions is found to be consistent with unity whereas a large jet suppression is observed for central Pb–Pb events with respect to peripheral events indicating the presence of a dense medium in these collisions. The jet spectra (or cross section) ratios indicate that the core of the jet remains unmodified even in the most central Pb–Pb collisions.

References

[1] S. D. Ellis, Z. Kunszt and D. E. Soper, *Phys. Rev. Lett.* **69** 3615 (1992).

[2] K. C. Zapp, F. Krauss and U. A. Wiedemann, *JHEP* **1303** 080 (2013).

[3] A. Majumder and M. Van Leeuwen, *Prog. Part. Nucl. Phys.* **A66** 41 (2011).

[4] ALICE Collaboration, *JINST* **3** S08002 (2008).

[5] ALICE Collaboration, *Int. J. Mod. Phys.* **A29** 1430044 (2014).

[6] ALICE Collaboration, *JINST* **5** P03003 (2010).

[7] ALICE Collaboration, CERN-LHCC-2004-025 *https://cds.cern.ch/record/781854* (2004).

[8] ALICE Collaboration, *Phys. Lett.* **B 722** 262 (2013).

[9] ALICE Collaboration, *Phys.Rev.* **D91** 112012 (2015).

[10] ALICE Collaboration, *Phys. Lett.* **B749**, 68 (2015).

[11] ALICE Collaboration, *JHEP* **03**, 013 (2014).

[12] ALICE Collaboration, CERN-LHCC-2008-014 *https://cds.cern.ch/record/1121574* (2008).

[13] J. Alme, Y. Andres, H. Appelshauser, S. Bablok, N. Bialas, et al., *Nucl. Instrum. Meth.* **A622** 316 (2010).

[14] M. Cacciari, G. P. Salam and G. Soyez, *JHEP* **0804** 063 (2008).

[15] S. Catani, Y. L. Dokshitzer, M. Seymour and B. Webber, *Nucl. Phys.* **B406** 187 (1993).

[16] S. D. Ellis and D. E. Soper, *Phys.Rev.* **D48** 3160 (1993).

[17] G. D Agostini, *Nucl. Instrum. Meth.* **A362** 487 (1995).

[18] A. Hocker and V. Kartvelishvili, *Nucl. Instrum. Meth.* **A372** 469 (1996).

[19] T. Sjostrand, S. Mrenna and P. Z. Skands, *JHEP* **0605** 026 (2006).

[20] R. Brun, F. Carminati and S. Giani, CERN-W5013, CERN-W-5013, *https://cds.cern.ch/record/1082634*.

[21] G. Soyez, *Phys. Lett.* **B698** 59 (2011).